Molecular Biology of the Cell
Vol. 20, 3888–3895, September 1, 2009

Caenorhabditis elegans FOS-1 and JUN-1 Regulate *plc-1* Expression in the Spermatheca to Control Ovulation

Susan M. Hiatt,* Holli M. Duren,* Y. John Shyu,* Ronald E. Ellis,† Naoki Hisamoto,‡ Kunihiro Matsumoto,‡ Ken-ichi Kariya,§ Tom K. Kerppola,‖ and Chang-Deng Hu*

*Department of Medicinal Chemistry and Molecular Pharmacology, School of Pharmacy and Pharmaceutical Sciences, Purdue University, West Lafayette, IN 47907; †Department of Molecular Biology, School of Osteopathic Medicine, University of Medicine and Dentistry of New Jersey, Stratford, NJ 08084; ‡Division of Biological Science, Graduate School of Science, Institute for Advanced Research, Nagoya University, Chikusa-ku, Nagoya 464-8602, Japan; §Division of Cell Biology, Graduate School of Medicine, University of the Ryukyus, Nishihara-cho, Okinawa 903-0215, Japan; and ‖Howard Hughes Medical Institute and Department of Biological Chemistry, University of Michigan Medical School, Ann Arbor, MI 48109

Submitted August 13, 2008; Revised June 17, 2009; Accepted June 23, 2009
Monitoring Editor: William P. Tansey

Fos and Jun are components of activator protein-1 (AP-1) and play crucial roles in the regulation of many cellular, developmental, and physiological processes. *Caenorhabditis elegans fos-1* has been shown to act in uterine and vulval development. Here, we provide evidence that *C. elegans fos-1* and *jun-1* control ovulation, a tightly regulated rhythmic program in animals. Knockdown of *fos-1* or *jun-1* blocks dilation of the distal spermathecal valve, a critical step for the entry of mature oocytes into the spermatheca for fertilization. Furthermore, *fos-1* and *jun-1* regulate the spermathecal-specific expression of *plc-1*, a gene that encodes a phospholipase C (PLC) isozyme that is rate-limiting for inositol triphosphate production and ovulation, and overexpression of PLC-1 rescues the ovulation defect in *fos-1(RNAi)* worms. Unlike *fos-1*, regulation of ovulation by *jun-1* requires genetic interactions with *eri-1* and *lin-15B*, which are involved in the RNA interference pathway and chromatin remodeling, respectively. At least two isoforms of *jun-1* are coexpressed with *fos-1b* in the spermatheca, and different AP-1 dimers formed between these isoforms have distinct effects on the activation of a reporter gene. These findings uncover a novel role for FOS-1 and JUN-1 in the reproductive system and establish *C. elegans* as a model for studying AP-1 dimerization.

INTRODUCTION

Ovulation is a tightly regulated rhythmic program. Because the nematode *Caenorhabditis elegans* is transparent and genetically tractable, it has become a model for studying this program. In *C. elegans*, an ovulation cycle begins as sperm signal the most proximal oocyte (the −1 oocyte) to mature. A critical component of this signal is major sperm protein (MSP), which binds the VAB-1 Eph receptor protein tyrosine kinase on oocytes and sheath cells (Miller *et al*., 2001, 2003). The MSP signal promotes oocyte maturation and sheath cell contractions. The oocyte then undergoes nuclear envelope breakdown (NEBD) and cortical rearrangement, and signals sheath cells via the epidermal growth factor-like ligand, LIN-3, to increase the strength and frequency of their contractions. When these contractions are coupled with dilation of the distal spermathecal valve, the mature oocyte is ovulated into the spermatheca for fertilization (McCarter *et al*., 1997, 1999). After fertilization, the spermatheca-uterine valve dilates so that the new egg can pass into the uterus (Figure 1A).

This article was published online ahead of print in *MBC in Press* (http://www.molbiolcell.org/cgi/doi/10.1091/mbc.E08–08–0833) on July 1, 2009.

Address correspondence to: Chang-Deng Hu (cdhu@pharmacy.purdue.edu).

Genetic analyses revealed that the inositol triphosphate (IP_3) signaling pathway plays a critical role in ovulation, because sheath cell contractions, distal spermathecal valve dilation, and spermatheca-uterine valve dilation are all controlled by IP_3-induced calcium release (Clandinin *et al*., 1998; Bui and Sternberg, 2002; Kariya *et al*., 2004; Yin *et al*., 2004) (Figure 1B). IP_3 is produced in sheath cells and spermathecal cells by the catalytic activity of the phospholipase C (PLC) enzymes PLC-3, PLC-1, or both. Levels of IP_3 can be reduced by IP_3 kinase let-23 fertility effector/regulator (LFE-2) or type I polyphosphate 5-phosphatase (IPP-5) (Clandinin *et al*., 1998; Bui and Sternberg, 2002; Kariya *et al*., 2004; Yin *et al*., 2004). Thus, loss-of-function mutations in *lfe-2* or *ipp-5* increase IP_3 concentration and suppress the ovulation defect caused by *lin-3* mutations (Clandinin *et al*., 1998; Bui and Sternberg, 2002). In addition, a gain-of-function mutation in *itr-1*, the IP_3 receptor, sensitizes it to Ca^{2+}, which also rescues the ovulation defects caused by mutants for the LIN-3 signal (Clandinin *et al*., 1998).

Fos and Jun are members of the activator protein-1 (AP-1) family, which constitutes an important subset of basic region leucine zipper (bZIP) transcription factors (Karin *et al*., 1997; Wagner, 2001). AP-1 proteins function as homodimers or heterodimers that bind DNA and regulate transcription of target genes. Genetic and biochemical studies have demonstrated that AP-1 proteins are critical regulators of many cellular and developmental processes, including growth,

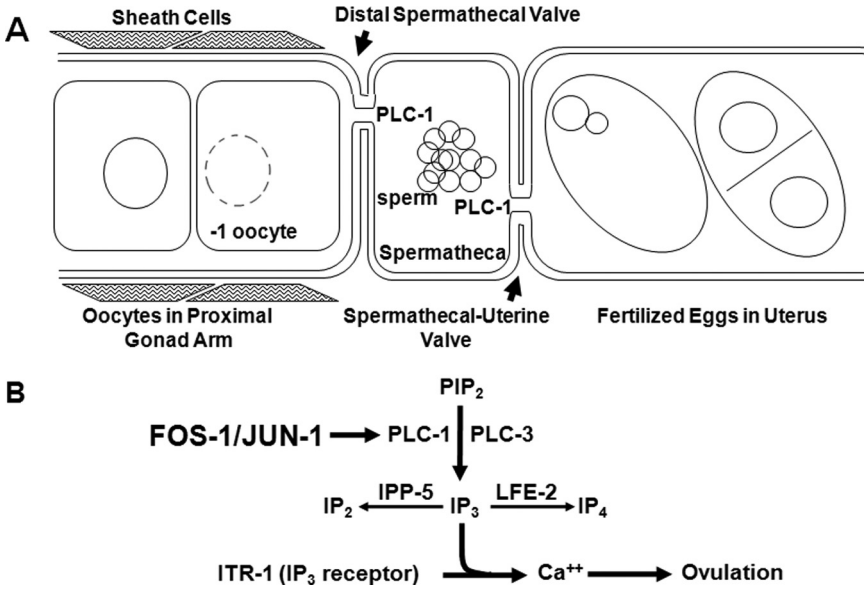

Figure 1. Regulation of ovulation by IP_3 signaling. (A) Outline of ovulation control in *C. elegans*. Ovulation is coordinated by sheath cell contractions and distal spermathecal valve dilation. These steps are controlled by the rate-limiting enzymes PLC-3 and PLC-1, respectively, which produce IP_3, thereby causing an increase in calcium concentration. (B) Genetic regulation of IP_3 concentration in sheath cells and spermathecal cells. This study demonstrates that *C. elegans* FOS-1 and JUN-1 regulate PLC-1 expression in the spermatheca and control distal spermathecal valve dilation.

differentiation, apoptosis, and stress responses (Karin *et al.*, 1997).

Recent studies in *C. elegans* showed that FOS-1A, one of the two isoforms of the *C. elegans* Fos homologue, regulates the development of the reproductive system, including anchor cell invasion and development of the uterus (Sherwood *et al.*, 2005; Oommen and Newman, 2007). However, knockdown of *fos-1* by RNA interference (RNAi) or deletion of *fos-1* also causes sterility (Oommen and Newman, 2007), which implies that *fos-1* plays additional roles in reproduction. Here, we show that FOS-1B regulates spermathecal valve dilation by controlling *plc-1* expression (Figure 1B). We also demonstrate that the *C. elegans* Jun homologue participates in this process. However, JUN-1 has a milder phenotype, and genetic evidence suggests that its role in ovulation is influenced by mutations in genes involved in the RNAi pathway and chromatin remodeling.

MATERIALS AND METHODS

Strains

Some nematode and *Escherichia coli* strains were provided by the *Caenorhabditis* Genetics Center (CGC, University of Minnesota, Minneapolis, MN), which is funded by the National Institutes of Health National Center for Research Resources. These reagents include OP50 and HT115(DE3) *Escherichia coli*, and the following nematode strains: wild-type N2, SU93 (*ajm-1::gfp*), NL2098 *rrf-1(pk1417)* I, NL2099 *rrf-3(pk1426)* II, KP3948 *eri-1(mg366)* IV; *lin-15B(n744)* X, PS2286 *unc-38(x20); lfe-2(sy326)* I, ZZ20 *unc-38(x20)* I, PK2368 *itr-1(sy327); unc-24(e138*) IV, CB138 *unc-24(e138)* IV, PS3653 *ipp-5(sy605*) X, VC1200 *jun-1(gk557)*, and PD8120 *smg-1(cc546)* I. *ipp-5::gfp*, *plc-3::gfp* and two *itr-1::gfp* strains were kindly provided by P. Sternberg (California Institute of Technology), K. Strange (Vanderbilt University), and H. Baylis (University of Cambridge), respectively.

Feeding RNAi

cDNAs encoding the bZIP region of *fos-1* and *jun-1*, full-length *fog-3*, exons 1 through 4 of *unc-112*, exons 1-7 of *eri-1a*, and the first 1 kb of the 5′ end of *lin-15B* were cloned into the feeding RNAi vector pPD129.36 (Timmons and Fire, 1998). Feeding RNAi was performed as described previously (Kamath *et al.*, 2001). In brief, HT115(DE3) *E. coli* were transformed with plasmid and grown 8 h at 37°C in Luria Broth containing ampicillin (100 μg/ml) and tetracycline (15 μg/ml). RNAi plates containing ampicillin (50 μg/ml), tetracycline (15 μg/ml), and isopropyl β-D-thiogalactoside (1 mM) were seeded with 200 μl of bacteria and incubated at 37°C overnight. Adult N2 worms were added and allowed to lay eggs for 48 h at 20°C. Phenotypes of F1 progeny were scored after an additional 24–48 h. *eri-1;lin-15B* worms were allowed to lay eggs for 72 h or were not removed until analysis of offspring.

Genetic Interactions between jun-1 and eri-1 or lin-15B

The homozygous double mutant *jun-1(gk557);lin-15B(n744*) X was made and confirmed by genotyping with polymerase chain reaction (PCR). RNAi in the background of various strains was performed as described above. Sterility was defined as the absence of fertilized eggs in the uterus.

4,6-Diamidino-2-phenylindole (DAPI) Staining

Fixation and staining were performed as described previously (Francis *et al.*, 1995), with slight modifications. In brief, a 60-mm plate of worms was rinsed twice with M9 buffer and then fixed in 3% fresh paraformaldehyde for 1 h. After two washes with phosphate-buffered saline containing 0.1% Tween 20 (PBST), worms were fixed in cold methanol at −20°C for 10 min. After two additional PBST washes, samples were incubated with 100 ng/ml DAPI in PBST for 10 min, washed, and mounted on slides. Images were captured using a Photometrics CoolSNAP ES digital camera (Roper Scientific, Tucson, AZ) controlled by MetaMorph version 6.2 software (Molecular Devices, Sunnyvale, CA) by using DAPI filters from Chroma Technology (Brattleboro, VT).

Time-Lapse Analysis of First Ovulations

Sheath cell contractions and spermathecal valve dilation studies were performed as described previously (Yin *et al.*, 2004). In brief, vector control or RNAi-treated adult worms were anesthetized in tricaine (0.1%) and tetramisole (0.01%) in M9 for 30–50 min. Worms were examined as described above, and images were acquired once per second for up to 45 min total. Time zero for each image was set to the completion of entry of the oocyte into the spermatheca. Ovulatory contractions consisted of the average contractions per minute of the three minutes preceding entry of the oocyte (−3 to −1). Basal contractions were averaged from 10 to 5 min before ovulation (−10 to −5). For *fos-1(RNAi)* worms, ovulatory contractions are maximal sheath contractions at the time of oocyte maturation, as evidenced by NEBD and cortical rearrangement. This "rounding" effect is consistent with that seen in the −3 to −1 time point for vector-treated worms. Contractions in each one minute time frame were counted at least three times and averaged.

Effect of fos-1 and jun-1 RNAi on plc-1:: gfp Expression in the Spermatheca

RNAi was performed as described above using the transgenic line expressing a *plc-1::gfp* reporter as described previously (Kariya *et al.*, 2004). To quantify fluorescence intensity in the spermatheca of young adult F1 worms, regions of interest (average, 11.4) were selected in each spermatheca, and the average fluorescence intensity was calculated (average, 7.2 spermathecae per RNAi treatment) using microscopy setup described above with green fluorescent protein (GFP) filters. A Student's *t* test was used to compare average fluorescence intensities between samples and to determine statistical significance.

Isolation of fos-1(km30) Deletion Mutant

The deletion mutant *fos-1(km30)* was generated by TMP/UV (Gengyo-Ando and Mitani, 2000) and isolated using sib-selection. Screening was performed using gene-specific primers as follows: external left, 5′-GTAAGCCAAATAG-

GAAAATTACGGT-3′; external right, 5′-CTCGATTTTTGGAATCTGAAG-TAAA-3′; internal left, 5′-TAATTTACATTAGGTTTGCCGACAT-3′; and internal right, 5′-AAATGAATGTACTCACTTTGCGTTC-3′.

Direct sequencing of the PCR products verified the deleted region. These deletion mutants were backcrossed more than twice to animals of a wild-type N2 background.

Expression Analysis of fos-1b and jun-1 Isoforms

Genomic DNA upstream of the transcriptional start sites of *fos-1b* (3.4 kb), *jun-1abc* (296 base pairs), *jun-1d* (296 base pairs), *jun-1e* (222 base pairs), and *jun-1f* (444 base pairs) were cloned into pPD95.70 (Fire lab *C. elegans* Vector Kit 1995 [www.addgene.org]). At least three independent transgenic lines were obtained following injection of each plasmid (10 ng/μl) and the *rol-6(su1006)* (100 ng/μl) marker. Observation of GFP expression and image acquisition were performed as described above.

Luciferase Reporter Gene Assay

Reporter assays were carried out in COS-1 cells essentially the same as described previously (Liu *et al*., 2006), by using 0.5 μg of plasmid encoding FOS-1B, JUN-1A, and/or JUN-1D, and assayed for luciferase activity 24 h after transfection. Statistical analysis of activation due to FOS-1B, JUN-1A, or both was performed using an ANOVA. Inhibition of FOS-1B and JUN-1A transactivation by JUN-1D also was analyzed using a two-way ANOVA.

Accession Numbers

National Center for Biotechnology Information accession numbers for cDNA sequences of *jun-1a-f* isoforms are EU553920, EU553921, EU553922, EU553923, EU553924, and EU553925, respectively.

fos-1 RNAi Phenotypes Rescued by PLC-1 Overexpression

Transgenic lines expressing a previously isolated PLC-1 (Shibatohge *et al*., 1998) driven under the heat shock promoter *hsp-16.41* were constructed. The expressed PLC-1 protein (residues 88–1853) contains intact X, Y, C2, RA1, and RA2 domains but lacks the N-terminal 87 residues. Rescue experiments were performed exactly the same as the RNAi experiments except that when F1 worms reached the larval stage 4, they were heat shocked at 33°C for 2 h to induce the expression of PLC-1. A second 30-min heat shock was performed 12 h later, followed by phenotypic analysis. The endomitotic oocytes (Emo) phenotype was defined as the accumulation of endomitotic oocytes in the proximal gonad by differential interference contrast (DIC) microscopy and confirmed by DAPI staining. Any worm showing Emo in one or both of the two proximal gonads was scored as Emo.

RESULTS

Knockdown of fos-1 and jun-1 Causes Sterility

In mammals, Fos and Jun are involved in multiple processes, including development, differentiation, apoptosis, and stress responses. To see whether the *C. elegans* homologue of Fos, *fos-1*, is also pleiotropic, we used feeding to perform RNAi in N2 worms (Kamath *et al*., 2001; Timmons *et al*., 2001). To knock down both isoforms of *fos-1*, we targeted the shared bZIP-encoding region. Knockdown of *fos-1* resulted in F1 progeny with several phenotypes, including sterility (95.1%), a protruding vulva (13.8%), and exploded through the vulva (4.6%) (Table 1). These observations are consistent with results from several genome-wide RNAi screens and the analysis of *fos-1(ar105)*, an allele that deletes only *fos-1a* (Kamath *et al*., 2003; Simmer *et al*., 2003; Rual *et al*., 2004; Sherwood *et al*., 2005; Oommen and Newman, 2007).

Like mammalian and *Drosophila* Fos and Jun proteins, *C. elegans* FOS-1 and JUN-1 form heterodimers (Hiatt *et al*., 2008; Shyu *et al*., 2008). To see whether *C. elegans jun-1* has the same role as *fos-1*, we performed RNAi in the wild type and failed to observe any phenotype in the F1 progeny, possibly because *jun-1* mRNA was not eliminated (unpublished observations). Thus, we performed similar experiments in two RNAi-sensitive strains. In *rrf-3(pk1426); jun-1(RNAi)* worms, we observed an egg-laying phenotype and some distal tip cell migration defects, but minimal sterility. However, in *jun-1(RNAi); eri-1(mg366); lin-15B(n744*) worms, we saw phenotypes similar to those caused by *fos-1* RNAi (Table 1). Together, these results show that *fos-1* and *jun-1* have multiple, overlapping functions in the reproductive system.

Table 1. *fos-1* and *jun-1* are necessary for fertility and *fos-1* functions in the soma

Strain	RNAi treatment (n)	Ste (%)	Pvl (%)	Exp (%)
N2	Vector (564)	1.2	0.2	0.0
N2	*fos-1* (348)	95.1	13.8	4.6
N2	*jun-1* (670)	1.7	2.2	0.2
N2	*fog-3* (208)	99.0	N.D.	N.D.
eri-1(mg366); lin-15B(n7444)	Vector (92)	6.5	4.4	0.0
eri-1(mg366); lin-15B(n7444)	*fos-1* (34)	97.1	94.1	5.9
eri-1(mg366); lin-15B(n7444)	*jun-1* (92)	93.5	35.9	10.9
rrf-1(pk1417)	Vector (247)	0.0	N.D.	N.D.
rrf-1(pk1417)	*fos-1* (140)	11.4	N.D.	N.D.
rrf-1(pk1417)	*fog-3* (188)	99.5	N.D.	N.D.

Exp, exploded through vulva; N.D., not determined; Pvl, protruding vulva; Ste, sterile.

Number of worms observed is in parentheses.

fos-1 and jun-1 Are Required for Ovulation

The high penetrance of the sterile phenotype in *fos-1(RNAi)* and *jun-1(RNAi); eri-1(mg366); lin-15B(n744)* worms prompted us to ask how *C. elegans* AP-1 proteins promote fertility. When we examined gonad morphology and germ cell development in younger animals, we found that *fos-1(RNAi)* worms seemed normal before ovulation began and did not show an obvious oogenesis defect, which is different from *fos-1* deletion alleles *fos-1(ar105)* and *fos-1(km30*) (see the following sections for details). However, the oocytes failed to enter the spermatheca in almost all of the young adults examined (93%; n = 79). Consequently, these worms accumulated Emo in the proximal gonad (Figure 2, C and D), a phenomenon that occurs when oocytes mature but are not ovulated or fertilized (Iwasaki *et al*., 1996). We observed a similar Emo phenotype in *jun-1(RNAi); eri-1(mg366); lin-15B(n744*) worms (Figure 2, G and H).

FOS-1 Acts in the Soma to Regulate Ovulation

The Emo phenotype is characteristic of an ovulation defect. Ovulation relies on proper signaling and function by sperm and oocytes in the germ line, by sheath cells and spermathecal valve cells in the soma. To determine which of these cells were responsible for the ovulation defect in *fos-1(RNAi)* worms, we used *rrf-1(pk1417)* mutants, which are deficient in somatic RNAi (Sijen *et al*., 2001). We found that *rrf-1(pk1417); fos-1(RNAi)* worms showed much less sterility than *fos-1(RNAi)* in N2 worms (Table 1). This result supports the hypothesis that *fos-1* acts in the soma to regulate ovulation. By contrast, sterility resulting from the knockdown of *fog-3*, a gene necessary for spermatogenesis (Ellis and Kimble, 1995) was not rescued in *rrf-1(pk1417)* worms. Thus, RNA interference is still functional in the germ line of this strain (Table 1).

FOS-1 Controls the Dilation of the Distal Spermathecal Valve

The somatic tissues involved in ovulation include both sheath cells and the distal spermatheca (McCarter *et al*., 1997, 1999). To see whether the defects in the *fos-1(RNAi)* worms were due to inadequate sheath cell contractions or to improper dilation of the distal spermathecal valve, we re-

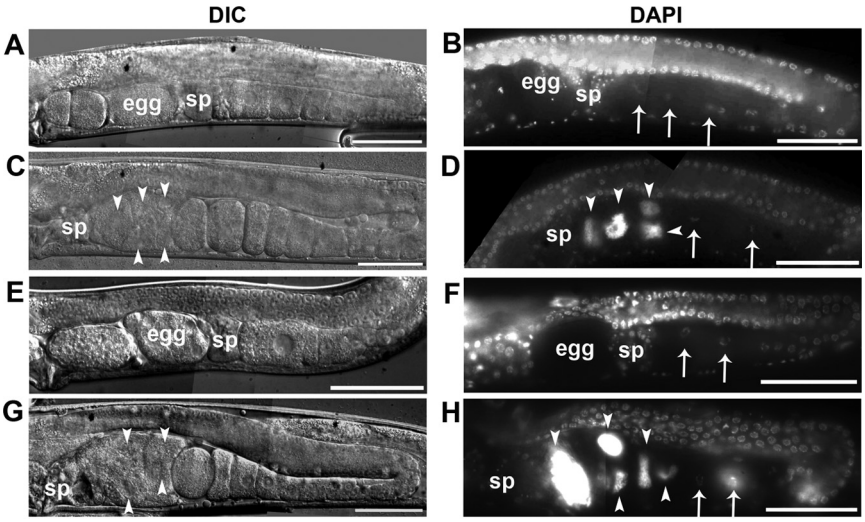

Figure 2. *fos-1* and *jun-1* are necessary for ovulation. Shown are representative DIC (left) and DAPI (right) images of worms treated with vector only (A and B) and *fos-1* RNAi (C and D) in N2, or vector only (E and F) and *jun-1* RNAi (G and H) in the RNAi sensitive strain *eri-1(mg366); lin15B(n744)*. Endomitotic oocytes are indicated by arrowheads, and nuclei of oocytes are indicated with arrows. sp, spermatheca. Bar, 50 μm.

corded these processes in living animals. Because endomitotic oocytes trapped in the proximal gonad obscure sheath cell contractions (Yin *et al*., 2004), we examined only the first ovulation in *fos-1(RNAi)* worms, using time-lapse microscopy (Supplemental Figure 1A and Supplemental Video 1). This time-lapse imaging also allowed the observation of other critical steps in ovulation, including oocyte maturation (as characterized by nuclear envelope breakdown and cortical rearrangement) and spermathecal valve dilation. In control worms, ovulations progressed normally (n = 5 animals), leading to the movement of oocytes into the spermatheca and the release of fertilized eggs into the uterus. However, all oocytes in *fos-1(RNAi)* worms failed to enter the spermatheca, even though oocyte maturation occurred normally (n = 4 animals; Supplemental Video 1). Quantification of sheath cell contractions indicated that there was only a slight difference in basal and ovulatory sheath cell contractions in *fos-1(RNAi)* worms when compared with vector controls (Supplemental Figure 1B). Because even untreated *eri-1(mg366); lin-15B(n744)* animals have reduced brood sizes and some ovulation defects (unpublished observations), we did not record ovulations in *jun-1(RNAi); eri-1(mg366); lin-15B(n744)* worms.

To see whether the lack of spermathecal valve dilation in *fos-1(RNAi)* worms was due to defects in spermathecal development, we performed *fos-1* RNAi in a strain that expresses GFP in spermathecal cells (Mohler *et al*., 1998; Michaux *et al*., 2001). Knockdown of *fos-1* in these animals did not cause detectable changes in the expression or localization of the *ajm-1::gfp* reporter in the spermatheca (data not shown). These results suggest that the primary defect in *fos-1* and *jun-1* RNAi-treated worms is a failure in distal spermathecal valve dilation.

fos-1 and jun-1 Deletion Mutants Exhibit Multiple Defects in the Reproductive System

To confirm the RNAi results, we isolated *fos-1(km30)*, which deletes an exon encoding part of the bZIP region, which is shared by FOS-1A and FOS-1B. The *fos-1(km30)* homozygotes showed severe defects in oocyte development, which prevented us from analyzing ovulation. However, *fos-1(km30)* heterozygotes displayed several phenotypes associated with reproduction, including sterility (11%), a protruding vulva (8%), a ruptured gonad (3%), the presence of debris or torn oocytes in the spermatheca (28%) and uterus (22%), and unfertilized oocytes in the uterus (11%) (n = 36). Thus, *fos-1* regulates many developmental and physiological processes in the reproductive system.

We also studied *jun-1*(*gk557*), which deletes the bZIP-coding region (*C. elegans* Gene Knockout Consortium). Reverse transcription-PCR analyses verified the absence of all isoforms (data not shown). Although *jun-1(gk557)* animals showed multiple defects in the reproductive system and had a reduced brood size, we only observed 5.1% sterility (Supplemental Table 2). Thus, *jun-1* and *fos-1* have overlapping phenotypes, but they are not identical in their effects on reproduction.

The ovulation defect we observed in *jun-1(RNAi); eri-1(mg366); lin-15B(n744)* worms might have been due to two distinct causes—the *eri-1(mg366); lin-15B(n744)* strain might enhance the effectiveness of RNAi against *jun-1* or *eri-1* and *lin-15B* might interact genetically with *jun-1* to regulate ovulation. Thus, we built *jun-1(gk557); lin-15B(n744)* double mutants for analysis. Because of decreased fertility, we could not build an *eri-1; lin-15b; jun-1* triple mutant. However, we did find that *jun-1(gk557); lin-15B(n744)* double mutants showed a high percentage of the Emo phenotype compared with either *jun-1(gk557)* or *lin-15B(n744)* single mutants (Supplemental Table 3). Thus, *jun-1* and *lin-15B* are partially redundant for the control of ovulation. In addition, we performed RNAi in *jun-1(gk557)* animals and observed that knockdown of *eri-1*, *lin-15B*, or both genes increased sterility (Supplemental Table 4). Together, these results strongly suggest that *jun-1* has multiple roles in the reproductive system. Furthermore, the regulation of ovulation by *jun-1* is influenced by the activities of *eri-1* and *lin-15B*.

fos-1 Genetically Interacts with Genes in the IP_3 Signaling Pathway

Genetic analysis demonstrated that the IP_3 signaling pathway is responsible for sheath cell contractions, distal spermathecal valve dilation, and spermatheca-uterine valve dilation through IP_3-induced calcium release (Clandinin *et al*., 1998; Bui and Sternberg, 2002; Kariya *et al*., 2004; Yin *et al*., 2004). Thus, we determined whether increased IP_3 levels could rescue the sterility induced by *fos-1* RNAi. We used three mutants that suppress the ovulation defects of *lin-3*

Table 2. Genetic interactions of *fos-1* with the IP_3 pathway

Strain	RNAi treatment (n)	Ste (%)	Unc (%)
N2	Vector (99)	0.0	N.D.
N2	*fos-1* (133)	90.8	N.D.
ipp-5(sy605)	Vector (98)	1.4	N.D.
ipp-5(sy605)	*fos-1* (68)	19.9*	N.D.
N2	Vector (634)	N.D.	0.0
N2	*unc-112* (427)	N.D.	100.0
ipp-5(sy605)	Vector (582)	N.D.	0.0
ipp-5(sy605)	*unc-112* (638)	N.D.	98.2
unc-24(e138)	Vector (201)	0.0	N.D.
unc-24(e138)	*fos-1* (178)	93.1	N.D.
unc-24(e138); itr-1(sy327)	Vector (191)	0.0	N.D.
unc-24(e138); itr-1(sy327)	*fos-1* (141)	90.8	N.D.
unc-38(x20)	Vector (211)	0.3	N.D.
unc-38(x20)	*fos-1* (128)	100.0	N.D.
unc-38(x20); lfe-2(sy326)	Vector (224)	0.3	N.D.
unc-38(x20); lfe-2(sy326)	*fos-1* (100)	97.4	N.D.

N.D., not determined; Ste, sterile; Unc, uncoordinated.

Number of worms observed is in parentheses. *$p < 0.05$ compared with *fos-1* RNAi in N2 worms.

mutants—a gain-of-function mutation in *itr-1*, and loss-of-function mutations in either *ipp-5* or *lfe-2*. We found that *ipp-5(sy605)* suppressed the sterility induced by *fos-1* RNAi, although neither *lfe-2(sy326)* nor *itr-1(sy327)* affected the phenotype. To exclude the possibility that the *ipp-5* mutation affects RNA interference, we performed RNAi against *unc-112*, a gene required for the assembly of muscle dense bodies and normal movement (Rogalski *et al*., 2000). We observed comparable levels of uncoordinated animals when RNAi was performed in wild type or *ipp-5(sy605)* worms (Table 2). Thus, the RNAi machinery is not compromised in *ipp-5* mutants, which implies that the defect in the dilation of the distal spermathecal valve in *fos-1(RNAi)* worms is due to decreased levels of IP_3 in the spermatheca.

fos-1 and jun-1 Regulate the Expression of plc-1 in the Spermatheca

Because AP-1 proteins are transcription factors, we suspected that *fos-1* and *jun-1* might regulate the expression of molecules in the IP_3 signaling pathway. Thus, we performed *fos-1* and *jun-1* RNAi in *plc-1*, *plc-3*, *ipp-5* and *itr-1* GFP reporter strains (Clandinin *et al*., 1998; Gower *et al*., 2001; Bui and Sternberg, 2002; Kariya *et al*., 2004; Yin *et al*., 2004). RNA interference against *fos-1* reduced the expression of *plc-1::gfp* in the spermatheca to 8.0% of the vector control, and RNA interference against *jun-1* reduced the expression of *plc-1::gfp* to 82.3% (Figure 3). This slight reduction of *plc-1::gfp* expression in the *jun-1(RNAi)* worms mirrors the low level of sterility found in these animals. However, *plc-1::gfp* expression in other tissues including the vulva, head, and tail seemed unaltered in all of these experiments. Furthermore, we saw no obvious changes in the expression of *plc-3::gfp*, *ipp-5::gfp* or *itr-1::gfp* in the spermatheca of *fos-1(RNAi)* or *jun-1(RNAi)* worms (unpublished observations). These results suggest that *fos-1* and *jun-1* regulate *plc-1* expression in the spermatheca.

To see whether down-regulation of *plc-1* transcription in the spermatheca was responsible for the ovulation defect in *fos-1(RNAi)* worms, we studied transgenic lines that can be induced to express PLC-1 by heat shock. In *fos-1(RNAi)* animals, overexpression of PLC-1 reduced the Emo phenotype by 58% (Table 3). However, overexpression of PLC-1 did not alter the protruding vulva phenotype. Thus, reduced expression of PLC-1 in the spermatheca is responsible for the ovulation defect in *fos-1(RNAi)* worms.

fos-1b, jun-1a-c and jun-1d Are Coexpressed in the Spermatheca

Two isoforms of *fos*-1 have been identified previously (Sherwood *et al*., 2005), and four isoforms of *jun-1* were pre-

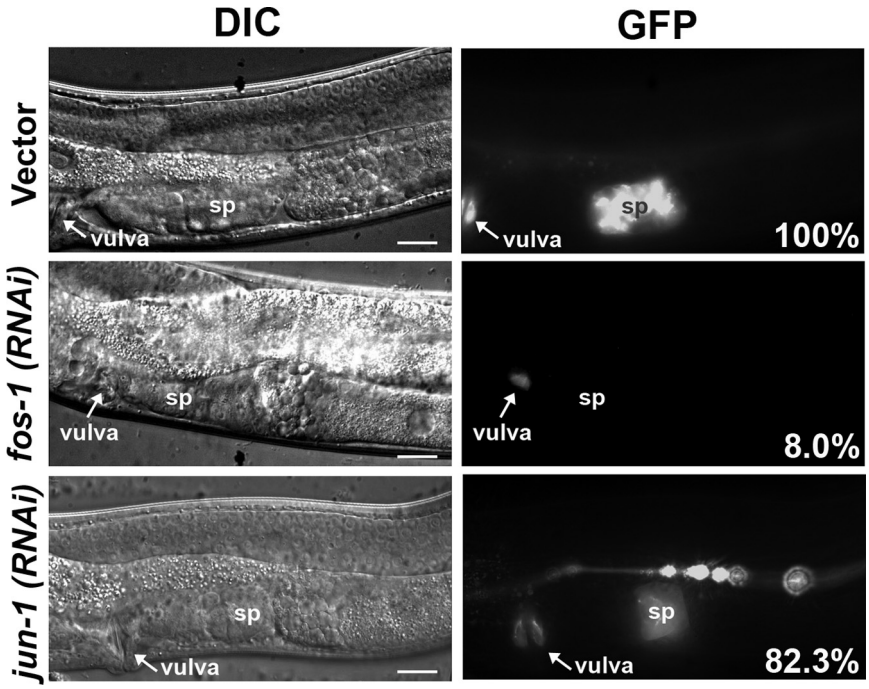

Figure 3. *fos-1* and *jun-1* regulate *plc-1* expression. (A) Effect of *fos-1* and *jun-1* RNAi on *plc-1::gfp* expression. Shown are DIC (left) and GFP (right) images of worms treated with vector only, *fos-1* RNAi, or *jun-1* RNAi. The numbers in the bottom right corners of the GFP images are quantified percentage of fluorescence intensity relative to vector-treated worms. Arrows indicate position of the vulva. Bar, 10 μm.

Table 3. Rescue of the ovulation defect in *fos-1(RNAi)* worms by *plc-1*

Strain	RNAi treatment (n)	Heat shock	Emo (%)
hs::plc-1	Vector (61)	No	0.0
hs::plc-1	*fos-1* (62)	No	83.4
hs::plc-1	*fos-1* (68)	Yes	35.5

hs, *hsp-16.41*.
Number of worms observed is in parentheses.

dicted (www.wormbase.org). To confirm these isoforms, we performed 5′ and 3′ rapid amplification of cDNA ends. These studies confirmed the expression of *fos-1a* and *fos-1b* and identified six isoforms of *jun-1*, which all share a common bZIP region (Supplemental Figure 2).

fos-1a is expressed in the anchor cell and uterus throughout gonadogenesis and regulates both anchor cell invasion and uterine development (Rogalski *et al*., 2000; Oommen and Newman, 2007). Although *fos-1b* is expressed in several tissues, its function had been unknown (Sherwood *et al*., 2005). To see whether *fos-1b* was expressed in the spermatheca, we used 3.4 kb of genomic DNA upstream of its transcriptional start site to build a GFP reporter plasmid. Transgenic worms carrying this plasmid expressed GFP in the spermatheca (Figure 4A).

Because *jun-1a* is the longest isoform, and differs only in exons 1 or 2 from *jun-1b* and *jun-1c*, we constructed a single transcriptional reporter for *jun-1a-c*. In addition, we created transcriptional reporters for *jun-1d*, *jun-1e*, and *jun-1f*. Examination of GFP expression in transgenic worms revealed that *jun-1a-c* and *jun-1d* are expressed in the spermatheca (Figure 4A), whereas *jun-1e* and *jun-1f* are not (unpublished observations). Hence, *fos-1b* and *jun-1a*, *b*, *c*, or *d* were likely to be responsible for the RNAi phenotypes we had observed.

The expression of multiple *jun-1* isoforms in the spermatheca suggested that these isoforms might interact to coordinate the transcription of target genes. For example, in mammals, the transcription of AP-1 target genes is subject to negative regulation by some AP-1 proteins that share essentially the same bZIP domain, such as JunB and JunD (Zenz and Wagner, 2006). In *C. elegans*, JUN-1D is one of three short isoforms that contain the bZIP domain and little else. Because the bZIP domains of JUN-1 and FOS-1 bind the consensus TPA response element (TRE) binding site as heterodimers as well as homodimers (unpublished observations), we examined the transcriptional potential of FOS-1B, JUN-1A, and JUN-1D. To do this, we used luciferase reporter gene assays in COS-1 cells. Although FOS-1B, JUN-1A, or JUN-1D alone showed minimal activation of the reporter gene, coexpression of JUN-1A with FOS-1B significantly activated the AP-1 reporter. However, coexpression of JUN-1D with FOS-1B had no effect (Figure 4B). Instead, coexpression of JUN-1D inhibited activation of the reporter by FOS-1B/JUN-1A when an equal amount of the plasmid encoding JUN-1D was cotransfected. These results suggest that JUN-1A and JUN-1D exhibit opposite effects on the activation of target genes when they form heterodimers with FOS-1B.

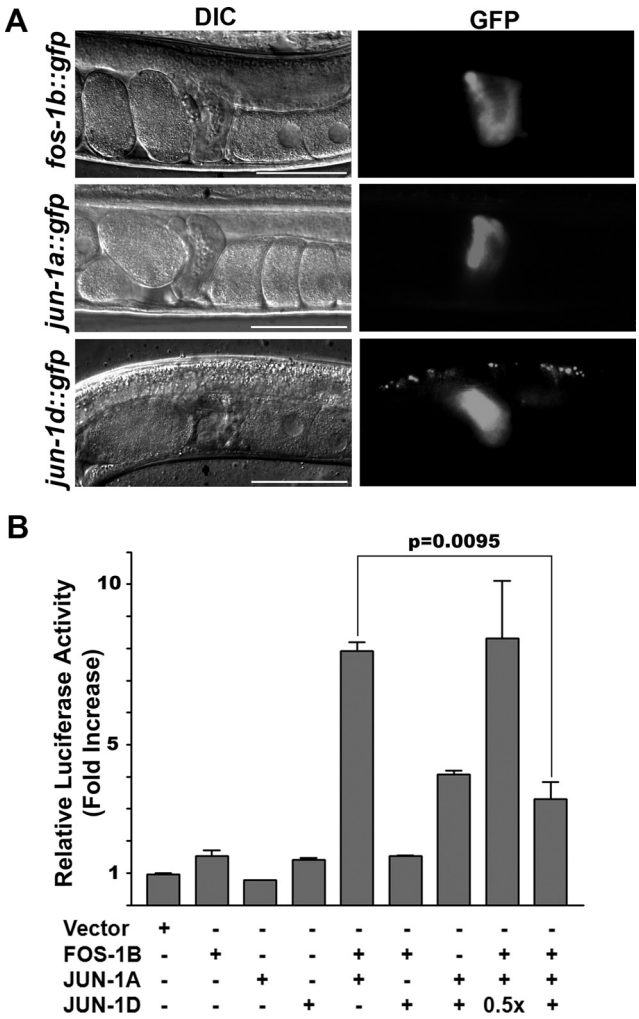

Figure 4. *fos-1b*, *jun-1abc*, and *jun-1d* are expressed in the spermatheca. (A) Expression of *fos-1b*, *jun-1abc*, and *jun-1d* in the spermatheca. Shown are DIC (left) and GFP (right) images in transgenic worms carrying the GFP reporters for *fos-1b*, *jun-1abc (jun-1a)*, or *jun-1d*. Scale, 50 μm. (B) Effect of FOS-1B, JUN-1A, and JUN-1D on activation of an AP-1 luciferase reporter that contains three TPA response elements (TGAGTCA). +, 0.5 μg; 0.5×, 0.25 μg.

DISCUSSION

FOS-1 and JUN-1 Regulate plc-1 Expression in the Spermatheca to Control Distal Spermathecal Valve Dilation

AP-1 family proteins regulate many physiological responses in cells and in animals, and the deregulation of these proteins is involved in numerous pathologies (Karin *et al*., 1997; Wagner, 2001). However, the role of AP-1 proteins in the reproductive system remains largely unexplored, due to the lack of appropriate model systems. Our findings that FOS-1 and JUN-1 control spermathecal valve dilation, along with the known role of FOS-1 in anchor cell invasion and cell fate specification in the uterus (Sherwood *et al*., 2005; Hwang *et al*., 2007; Oommen and Newman, 2007; Rimann and Hajnal, 2007; Sapir *et al*., 2007), establish *C. elegans* as a model for the control of reproduction by AP-1 proteins.

Spermathecal valve dilation is essential for successful ovulation. Genetic analysis showed that it depends on several genes that act in the IP_3 signaling pathway to control

calcium levels (Clandinin *et al*., 1998; Bui and Sternberg, 2002; Kariya *et al*., 2004; Yin *et al*., 2004). We present several lines of evidence that FOS-1 and JUN-1 regulate *plc-1* transcription specifically in the spermatheca. First, *fos-1b*, *jun-1a-c* and *jun-1d* are all coexpressed in the spermatheca, along with *plc-1*. Second, knockdown of *fos-1* or *jun-1* decreased expression of a *plc-1::gfp* reporter in the spermatheca, without affecting its expression in other tissues. Third, the lack of distal spermathecal valve dilation caused by *fos-1* RNAi was suppressed by *ipp-5(sy605)*, a mutant allele that increases IP_3 levels by inhibiting the metabolism of IP_3, but was not suppressed by *lfe-2(sy326)* or *itr-1(sy327)*. This pattern of suppression is identical to that observed for *plc-1* with these mutations (Kariya *et al*., 2004). Fourth, overexpression of PLC-1 rescued the Emo phenotype in *fos-1(RNAi)* worms. Thus, our studies provide a link between *fos-1/jun-1* and *plc-1* in *C. elegans*.

Other PLC isozymes in worms have been implicated in the regulation of all three major rhythmic programs—pharyngeal pumping, ovulation and defecation (Kariya *et al*., 2004; Yin *et al*., 2004; Espelt *et al*., 2005; Norman *et al*., 2005). Thus, it will be interesting to determine whether AP-1 proteins also regulate the transcription of any of these PLC isozymes. In mammals, AP-1 proteins regulate circadian rhythms by controlling the transcription of critical target genes (Kornhauser *et al*., 1992; Crosio *et al*., 2000; Hirayama *et al*., 2005), so the role of AP-1 proteins in rhythmic behaviors might be ancient.

Although we show that *fos-1* and *jun-1* regulate ovulation via *plc-1*, there might be additional target genes involved in ovulation. For example, that overexpressing PLC-1 in *fos-1(RNAi*) worms only partially rescues the ovulation defect and *fos-1* RNAi causes a slight reduction in sheath cell contractions could indicate that *fos-1* and *jun-1* control additional targets. This possibility is supported by the penetrance of the ovulation defect in *fos-1(RNAi)* worms, which is higher than that in *plc-1* deletion mutants (Kariya *et al*., 2004).

Chromatin Remodeling Influences Transcriptional Regulation of AP-1 Target Genes

In *C. elegans*, three classes of genes can interact to create a synthetic multivulval (SynMuv) phenotype (Fay and Yochem, 2007). Genetic and biochemical evidence suggests that these genes influence chromatin remodeling (Thomas *et al*., 2003; Ceol and Horvitz, 2004; Poulin *et al*., 2005; Cui *et al*., 2006; Harrison *et al*., 2006). It is interesting that *jun-1(RNAi)* animals only showed an ovulation defect in the strain *eri-1(mg366); lin-15B(n744)*. Although *eri-1* is an RNAse that influences RNA interference, *lin-15B* is a gene with SynMuvB activity (Wang *et al*., 2005). Furthermore, we found that a *lin-15B* mutation, *n744*, was sufficient for this interaction with *jun-1*. Finally, a general RNAi screen identified 57 genes, including *jun-1*, that interact with SynMuv genes like *lin-15B*, *lin-35* and *lin-37* (Ceron *et al*., 2007). Thus, a complex regulatory mechanism involving chromatin remodeling might influence the transcriptional regulation of *plc-1* by *jun-1*.

Knocking down *fos-1* in the wild type is sufficient to down-regulate *plc-1* transcription and to cause an ovulation defect, but the same is not true for *jun-1*. However, several observations support an alternative model. First, several JUN-1 isoforms are expressed in the spermatheca. Second, FOS-1B/JUN-1A positively regulates a reporter gene in tissue culture, but JUN-1D antagonizes this interaction. Thus, FOS-1/JUN-1A might promote transcription of *plc-1* in the spermatheca, and JUN-1D might block transcription. If correct, this model would explain the weak phenotype of *jun-1* deletion mutants, since both its positive and negative activities would be eliminated. In addition, this model implies that the enhancement of the ovulation defect seen in *jun-1(mg366); lin-15B(n744*) mutants could have been caused by a differential effect of chromatin alterations on the activity of the two JUN-1 isoforms. This inference is supported by the observation that knockdown of *jun-1* in the background of *lin-35* or *lin-37* mutations also causes sterility (Ceron *et al*., 2007). Further analysis of the interactions between *jun-1* and other SynMuv genes could provide insight into the transcriptional regulation of AP-1 target genes via chromatin remodeling.

AP-1 Dimerization in Transcriptional Regulation of Target Genes

AP-1 has been extensively studied over the past two decades. One challenge in the field is to assign specific cellular or developmental roles to individual AP-1 dimers. This has been impeded by the presence of multiple AP-1 proteins in mammals, allowing potential dimerization of any single AP-1 protein with several partners. These complexities contribute to functional complementation when only a single AP-1 gene is knocked out (Jochum *et al*., 2001). By contrast, model organisms with reduced genetic redundancy allow functional analysis of AP-1 dimers and their corresponding target genes, as shown by studies in *Drosophila* (Kockel *et al*., 2001; Ciapponi and Bohmann, 2002).

At least two different isoforms, *jun-1a* and *jun-1d*, are coexpressed with *fos-1b* in the spermatheca. Our proposal that multiple AP-1 dimers with distinct transcriptional potential could be formed in the spermatheca is based on this fact, and on the ability of the bZIP domains of FOS-1 and JUN-1 to form homodimers and heterodimers (unpublished observations). Furthermore, it is supported by the observation that JUN-1A and JUN-1D play opposite roles in activating an AP-1 reporter gene. We have identified four potential TRE sites in the promoter used for the *plc-1::gfp* reporter strain (unpublished observations). Thus, future characterization of the *plc-1* promoter and its regulation by different AP-1 proteins should show how these AP-1 proteins coordinate the transcription of *plc-1* in the spermatheca and could provide a model system for studying the interaction of different AP-1dimers on transcription.

ACKNOWLEDGMENTS

We thank the Hu laboratory for valuable discussions and critical reading of the manuscript, Apinya Suppatkul and Jonathan Smith for laboratory assistance, and Xuehong Deng for valuable support for the laboratory and for performing the luciferase reporter gene assays. We thank David Allen for video editing. We are indebted to the Strome laboratory for valuable discussions and to Susan Strome for critical reading and editing of the manuscript. We also thank the C.G.C., Paul Sternberg, Howard Baylis, and Kevin Strange for strains. S.M.H. was supported by the Purdue University Ross Fellowship and the Bilsland Dissertation Fellowship, R.E.E. was supported by a grant from the American Cancer Society, and C.D.H. was supported by a grant from the National Science Foundation.

REFERENCES

Bui, Y. K., and Sternberg, P. W. (2002). *Caenorhabditis elegans* inositol 5-phosphatase homolog negatively regulates inositol 1,4,5-triphosphate signaling in ovulation. Mol. Biol. Cell *13*, 1641–1651.

Ceol, C. J., and Horvitz, H. R. (2004). A new class of *C. elegans* synMuv genes implicates a Tip60/NuA4-like HAT complex as a negative regulator of Ras signaling. Dev. Cell *6*, 563–576.

Ceron, J., Rual, J. F., Chandra, A., Dupuy, D., Vidal, M., and van den Heuvel, S. (2007). Large-scale RNAi screens identify novel genes that interact with the *C. elegans* retinoblastoma pathway as well as splicing-related components with synMuv B activity. BMC Dev. Biol. *7*, 30.

Ciapponi, L., and Bohmann, D. (2002). An essential function of AP-1 heterodimers in *Drosophila* development. Mech. Dev. *115*, 35–40.

Clandinin, T. R., DeModena, J. A., and Sternberg, P. W. (1998). Inositol trisphosphate mediates a RAS-independent response to LET-23 receptor tyrosine kinase activation in *C. elegans*. Cell *92*, 523–533.

Crosio, C., Cermakian, N., Allis, C. D., and Sassone-Corsi, P. (2000). Light induces chromatin modification in cells of the mammalian circadian clock. Nat. Neurosci. *3*, 1241–1247.

Cui, M., Kim, E. B., and Han, M. (2006). Diverse chromatin remodeling genes antagonize the Rb-involved SynMuv pathways in *C. elegans*. PLoS Genet. *2*, e74.

Ellis, R. E., and Kimble, J. (1995). The *fog-3* gene and regulation of cell fate in the germ line of *Caenorhabditis elegans*. Genetics *139*, 561–577.

Espelt, M. V., Estevez, A. Y., Yin, X., and Strange, K. (2005). Oscillatory Ca^{2+} signaling in the isolated *Caenorhabditis elegans* intestine: role of the inositol-1,4,5-trisphosphate receptor and phospholipases C beta and gamma. J. Gen. Physiol. *126*, 379–392.

Fay, D. S., and Yochem, J. (2007). The SynMuv genes of *Caenorhabditis elegans* in vulval development and beyond. Dev. Biol. *306*, 1–9.

Francis, R., Barton, M. K., Kimble, J., and Schedl, T. (1995). *gld-1*, a tumor suppressor gene required for oocyte development in *Caenorhabditis elegans*. Genetics *139*, 579–606.

Gengyo-Ando, K., and Mitani, S. (2000). Characterization of mutations induced by ethyl methanesulfonate, UV, and trimethylpsoralen in the nematode *Caenorhabditis elegans*. Biochem. Biophys. Res. Commun. *269*, 64–69.

Gower, N. J., Temple, G. R., Schein, J. E., Marra, M., Walker, D. S., and Baylis, H. A. (2001). Dissection of the promoter region of the inositol 1,4,5-trisphosphate receptor gene, *itr-1*, in *C. elegans*: a molecular basis for cell-specific expression of IP3R isoforms. J. Mol. Biol. *306*, 145–157.

Harrison, M. M., Ceol, C. J., Lu, X., and Horvitz, H. R. (2006). Some *C. elegans* class B synthetic multivulva proteins encode a conserved LIN-35 Rb-containing complex distinct from a NuRD-like complex. Proc. Natl. Acad. Sci. USA *103*, 16782–16787.

Hiatt, S. M., Shyu, Y. J., Duren, H. M., and Hu, C. D. (2008). Bimolecular fluorescence complementation (BiFC) analysis of protein interactions in *Caenorhabditis elegans*. Methods *45*, 185–191.

Hirayama, J., Cardone, L., Doi, M., and Sassone-Corsi, P. (2005). Common pathways in circadian and cell cycle clocks: light-dependent activation of Fos/AP-1 in zebrafish controls CRY-1a and WEE-1. Proc. Natl. Acad. Sci. USA *102*, 10194–10199.

Hwang, B. J., Meruelo, A. D., and Sternberg, P. W. (2007). *C. elegans* EVI1 proto-oncogene, EGL-43, is necessary for Notch-mediated cell fate specification and regulates cell invasion. Development *134*, 669–679.

Iwasaki, K., McCarter, J., Francis, R., and Schedl, T. (1996). emo-1, a *Caenorhabditis elegans* Sec61p gamma homologue, is required for oocyte development and ovulation. J. Cell Biol. *134*, 699–714.

Jochum, W., Passegue, E., and Wagner, E. F. (2001). AP-1 in mouse development and tumorigenesis. Oncogene *20*, 2401–2412.

Kamath, R. S., *et al*. (2003). Systematic functional analysis of the *Caenorhabditis elegans* genome using RNAi. Nature *421*, 231–237.

Kamath, R. S., Martinez-Campos, M., Zipperlen, P., Fraser, A. G., and Ahringer, J. (2001). Effectiveness of specific RNA-mediated interference through ingested double-stranded RNA in *Caenorhabditis elegans*. Genome Biol. *2*, RESEARCH0002.

Karin, M., Liu, Z., and Zandi, E. (1997). AP-1 function and regulation. Curr. Opin. Cell Biol. *9*, 240–246.

Kariya, K., Bui, Y. K., Gao, X., Sternberg, P. W., and Kataoka, T. (2004). Phospholipase C epsilon regulates ovulation in *Caenorhabditis elegans*. Dev. Biol. *274*, 201–210.

Kockel, L., Homsy, J. G., and Bohmann, D. (2001). *Drosophila* AP-1, lessons from an invertebrate. Oncogene *20*, 2347–2364.

Kornhauser, J. M., Nelson, D. E., Mayo, K. E., and Takahashi, J. S. (1992). Regulation of jun-B messenger RNA and AP-1 activity by light and a circadian clock. Science *255*, 1581–1584.

Liu, H., Deng, X., Shyu, Y. J., Li, J. J., Taparowsky, E. J., and Hu, C. D. (2006). Mutual regulation of c-Jun and ATF2 by transcriptional activation and subcellular localization. EMBO J. *25*, 1058–1069.

McCarter, J., Bartlett, B., Dang, T., and Schedl, T. (1997). Soma-germ cell interactions in *Caenorhabditis elegans*: multiple events of hermaphrodite germline development require the somatic sheath and spermathecal lineages. Dev. Biol. *181*, 121–143.

McCarter, J., Bartlett, B., Dang, T., and Schedl, T. (1999). On the control of oocyte meiotic maturation and ovulation in *Caenorhabditis elegans*. Dev. Biol. *205*, 111–128.

Michaux, G., Legouis, R., and Labouesse, M. (2001). Epithelial biology: lessons from *Caenorhabditis elegans*. Gene *277*, 83–100.

Miller, M. A., Nguyen, V. Q., Lee, M. H., Kosinski, M., Schedl, T., Caprioli, R. M., and Greenstein, D. (2001). A sperm cytoskeletal protein that signals oocyte meiotic maturation and ovulation. Science *291*, 2144–2147.

Miller, M. A., Ruest, P. J., Kosinski, M., Hanks, S. K., and Greenstein, D. (2003). An Eph receptor sperm-sensing control mechanism for oocyte meiotic maturation in *Caenorhabditis elegans*. Genes Dev. *17*, 187–200.

Mohler, W. A., Simske, J. S., Williams-Masson, E. M., Hardin, J. D., and White, J. G. (1998). Dynamics and ultrastructure of developmental cell fusions in the *Caenorhabditis elegans* hypodermis. Curr. Biol. *8*, 1087–1090.

Norman, K. R., Fazzio, R. T., Mellem, J. E., Espelt, M. V., Strange, K., Beckerle, M. C., and Maricq, A. V. (2005). The Rho/Rac-family guanine nucleotide exchange factor VAV-1 regulates rhythmic behaviors in *C. elegans*. Cell *123*, 119–132.

Oommen, K. S., and Newman, A. P. (2007). Co-regulation by Notch and Fos is required for cell fate specification of intermediate precursors during *C. elegans* uterine development. Development *134*, 3999–4009.

Poulin, G., Dong, Y., Fraser, A. G., Hopper, N. A., and Ahringer, J. (2005). Chromatin regulation and sumoylation in the inhibition of Ras-induced vulval development in *Caenorhabditis elegans*. EMBO J. *24*, 2613–2623.

Rimann, I., and Hajnal, A. (2007). Regulation of anchor cell invasion and uterine cell fates by the *egl-43* Evi-1 proto-oncogene in *Caenorhabditis elegans*. Dev. Biol. *308*, 187–195.

Rogalski, T. M., Mullen, G. P., Gilbert, M. M., Williams, B. D., and Moerman, D. G. (2000). The UNC-112 gene in *Caenorhabditis elegans* encodes a novel component of cell-matrix adhesion structures required for integrin localization in the muscle cell membrane. J. Cell Biol. *150*, 253–264.

Rual, J. F., *et al*. (2004). Toward improving *Caenorhabditis elegans* phenome mapping with an ORFeome-based RNAi library. Genome Res. *14*, 2162–2168.

Sapir, A., Choi, J., Leikina, E., Avinoam, O., Valansi, C., Chernomordik, L. V., Newman, A. P., and Podbilewicz, B. (2007). AFF-1, a FOS-1-regulated fusogen, mediates fusion of the anchor cell in *C. elegans*. Dev. Cell *12*, 683–698.

Sherwood, D. R., Butler, J. A., Kramer, J. M., and Sternberg, P. W. (2005). FOS-1 promotes basement-membrane removal during anchor-cell invasion in *C. elegans*. Cell *121*, 951–962.

Shibatohge, M., Kariya, K., Liao, Y., Hu, C. D., Watari, Y., Goshima, M., Shima, F., and Kataoka, T. (1998). Identification of PLC210, a *Caenorhabditis elegans* phospholipase C, as a putative effector of Ras. J. Biol. Chem. *273*, 6218–6222.

Shyu, Y. J., Hiatt, S. M., Duren, H. M., Ellis, R. E., Kerppola, T. K., and Hu, C. D. (2008). Visualization of protein interactions in living *Caenorhabditis elegans* using bimolecular fluorescence complementation analysis. Nat. Protoc. *3*, 588–596.

Sijen, T., Fleenor, J., Simmer, F., Thijssen, K. L., Parrish, S., Timmons, L., Plasterk, R. H., and Fire, A. (2001). On the role of RNA amplification in dsRNA-triggered gene silencing. Cell *107*, 465–476.

Simmer, F., Moorman, C., Van Der Linden, A. M., Kuijk, E., Van Den Berghe, P. V., Kamath, R., Fraser, A. G., Ahringer, J., and Plasterk, R. H. (2003). Genome-Wide RNAi of *C. elegans* Using the Hypersensitive rrf-3 Strain Reveals Novel Gene Functions. PLoS Biol. *1*, E12.

Thomas, J. H., Ceol, C. J., Schwartz, H. T., and Horvitz, H. R. (2003). New genes that interact with *lin-35* Rb to negatively regulate the let-60 ras pathway in *Caenorhabditis elegans*. Genetics *164*, 135–151.

Timmons, L., Court, D. L., and Fire, A. (2001). Ingestion of bacterially expressed dsRNAs can produce specific and potent genetic interference in *Caenorhabditis elegans*. Gene *263*, 103–112.

Timmons, L., and Fire, A. (1998). Specific interference by ingested dsRNA. Nature *395*, 854.

Wagner, E. F. (2001). AP-1–Introductory remarks. Oncogene *20*, 2334–2335.

Wang, D., Kennedy, S., Conte, D., Jr., Kim, J. K., Gabel, H. W., Kamath, R. S., Mello, C. C., and Ruvkun, G. (2005). Somatic misexpression of germline P granules and enhanced RNA interference in retinoblastoma pathway mutants. Nature *436*, 593–597.

Yin, X., Gower, N. J., Baylis, H. A., and Strange, K. (2004). Inositol 1,4,5-trisphosphate signaling regulates rhythmic contractile activity of myoepithelial sheath cells in *Caenorhabditis elegans*. Mol. Biol. Cell *15*, 3938–3949.

Zenz, R., and Wagner, E. F. (2006). Jun signalling in the epidermis: from developmental defects to psoriasis and skin tumors. Int. J. Biochem. Cell Biol. *38*, 1043–1049.